

Lawrence Berkeley National Laboratory

Lawrence Berkeley National Laboratory

Title

Dynamics of Low Energy Electron Attachment to Formic Acid

Permalink

<https://escholarship.org/uc/item/5070j3wx>

Authors

Rescigno, Thomas N.
Trevisan, Cynthia S.
Orel, Ann E.

Publication Date

2006-04-03

Peer reviewed

Dynamics of low energy electron attachment to formic acid

T. N. Rescigno

Chemical Sciences, Lawrence Berkeley National Laboratory, One Cyclotron Road, Berkeley, CA 94720

C. S. Trevisan and A. E. Orel

Department of Applied Science, University of California, Davis, CA 95616

Low-energy electrons (<2 eV) can fragment gas phase formic acid (HCOOH) molecules through resonant dissociative attachment processes. Recent experiments have shown that the principal reaction products of such collisions are formate ions (HCOO^-) and hydrogen atoms. Using first-principles electron scattering calculations, we have identified the responsible negative ion state as a transient π^* anion. Symmetry considerations dictate that the associated dissociation dynamics are intrinsically polyatomic: a second anion surface, connected to the first by a conical intersection, is involved in the dynamics and the transient anion must necessarily deform to non-planar geometries before it can dissociate to the observed stable products.

PACS numbers: 34.80.Gs

The stunning demonstration by Boudaiffa *et al* [1] that single- and double-strand breaks in DNA can be produced by low-energy electrons has contributed to a renewed interest in “electron-driven processes” and, in particular, low-energy electron attachment processes involving biologically relevant species. Formic acid, the simplest of the organic acids, is interesting in this regard. In the 1980’s, it was identified as being present in the interstellar medium [2, 3] and it has been speculated that formic acid plays a role in the formation of simple biomolecules such as acetic acid and glycine.

There has been recent experimental work on dissociative electron attachment (DEA) to gas phase formic acid. The experiments [4, 5] show a strong peak in the DEA spectrum near 1.3 eV incident electron energy, with a width of ~ 0.5 eV, which correlates with production of formate (HCOO^-) anions. Interestingly, the experiments indicate that as a function of incident electron energy, DEA proceeds with an almost vertical onset that is close to the thermodynamic threshold for the process and also gives some indication of fine structure oscillations on the high-energy tail of the peak. Similar structure had been observed in earlier electron transmission experiments [6, 7] and there is also evidence that resonance structure is present in both the elastic [8] and the electron impact vibrational excitation cross sections [9, 10] for this molecule in the 1.5-2.0 eV energy range.

Previous theoretical work on electron interactions with formic acid is scarce. In their experimental study [5], the authors also carried out electronic structure calculations on the neutral molecule and, on the basis of an examination of its unoccupied (virtual) orbitals, concluded that a series of closely spaced overlapping negative ion resonances was involved in the DEA process. This notion was negated by Gianturco and Lucchese [11] who carried out electron scattering calculations using a purely

local potential model. Their calculations gave an isolated π^* shape resonance near 3.5eV, which they claimed was the probable precursor state for the metastable anion which dissociates to the experimentally observed fragments. However, since the calculations were carried out only at the equilibrium geometry of the target, their study gives no information about the dissociation pathway or the associated dynamics.

There are numerous examples of low-energy π^* shape resonances that occur in electron scattering by small, unsaturated molecules (N_2 , CO, CO_2 , H_2CO , C_2H_4 , C_2F_4) where the scattered electron is temporarily trapped in a localized, antibonding π orbital by tunneling through a centrifugal barrier. The energies and lifetimes of such resonances are usually sensitive to small changes in the length of the unstaurated bond and play a key role in vibrational excitation of the target molecule.

We have found, in calculations to be described below, that there is a negative ion π^* resonance in the case of the electron-formic acid system that falls within the appropriate experimentally observed energy range, so it is logical to assume that this resonance is in some way involved in the observed DEA channel. But there are several complicating factors. One obvious problem is that it is the OH bond that must be broken to form the formate anion (see Fig. 1) and not the carbonyl bond which initially traps the electron. There are also symmetry issues that argue against a simple interpretation of the experimental results. At its equilibrium geometry, formic acid is a planar molecule, belonging to the point group C_s . In planar geometry, its neutral and anion states can be classified either as A' or A'' , the latter being antisymmetric under reflection through the molecular plane. The formate anion has a closed-shell, planar (A') structure, and ground-state atomic hydrogen is A' , since it is, of course, 2S . Therefore, in planar geometry, $\text{H} + \text{HCOO}^-$ must

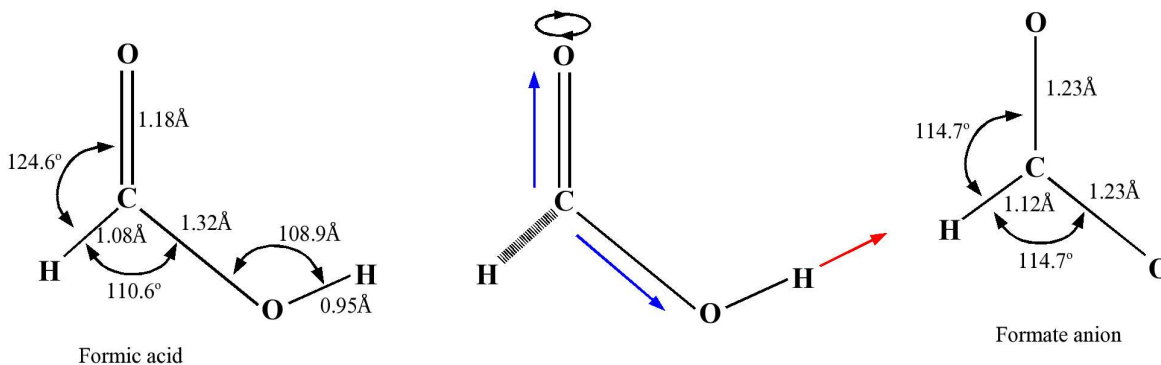


FIG. 1: (Color online) Equilibrium geometries of formic acid and formate anion, as well as negative ion intermediate. Angles are in degrees and distances are in units of angstroms, where $1\text{\AA}=10^{-10}\text{m}$. The arrows shown on the negative ion intermediate indicate a reaction path that involves first stretching the C=O and C-O bonds, followed by an out-of plane rotation (indicated by the circular arrow) of the CH bond (indicated by the thick line) and finally breaking of the OH bond.

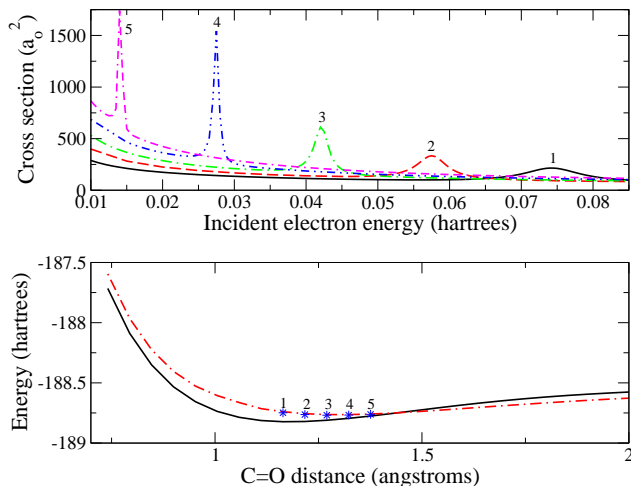


FIG. 2: (Color online) Fixed-nuclei cross sections and potential energy curves as a function of C=O distance in planar geometry. Upper panel: cross sections (right to left) starting with a C=O distance of 1.3\AA and increasing in increments of 0.0529\AA . Lower panel: potential energy curves for anion (dash-dot curve) and neutral target (solid curve). Numbered points on anion curve correspond to resonance energies obtained from cross sections (also numbered) shown in upper panel. Internuclear distances are given in angstroms. Cross sections are in units of a_0^2 where $a_0 = 5.2917721 \times 10^{-11}\text{m}$ is the Bohr radius. Energies are in units of hartrees, where one hartree = $4.359748 \times 10^{-18}\text{J}$.

have A' symmetry. On the other hand, capture of an electron into a π^* resonance orbital produces a negative ion state of A'' symmetry. Therefore, in order to produce A' fragments, the planar symmetry must be broken along the reaction path, allowing interaction with a second anion state that can dissociate to the observed fragments.

In this Letter, we report a series of calculations that elucidate the correct mechanism for DEA in formic acid.

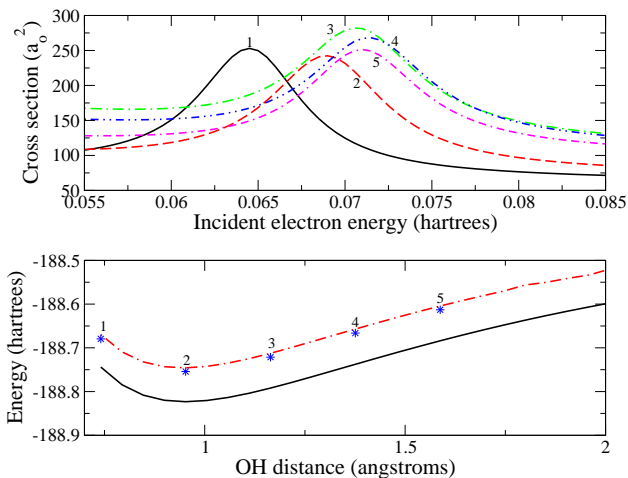


FIG. 3: (Color online) As in Fig. 2, for varying O-H distance in planar geometry. Upper panel: cross sections (1 through 5) starting with O-H distance of 0.74\AA and increasing in increments of 0.21\AA .

Our calculations show how this classic π^* resonance, initially localized on the C=O bond, ultimately leads to dissociation of the OH bond. The reaction occurs because there is more than one nuclear degree of freedom involved in the dissociation, which is an inherently polyatomic effect. For target geometries at which the anion is electronically unbound, its energy is complex-valued and it appears as a resonance in the fixed-nuclei $e^- + \text{HCOOH}$ elastic cross section. We have carried out a series of variational calculations employing the complex Kohn method [12] to characterize the resonance at a number of different geometries. The target molecule was described by a self-consistent field (SCF) wave function and target response (short-range correlation and long-range polarization) was accounted for by including

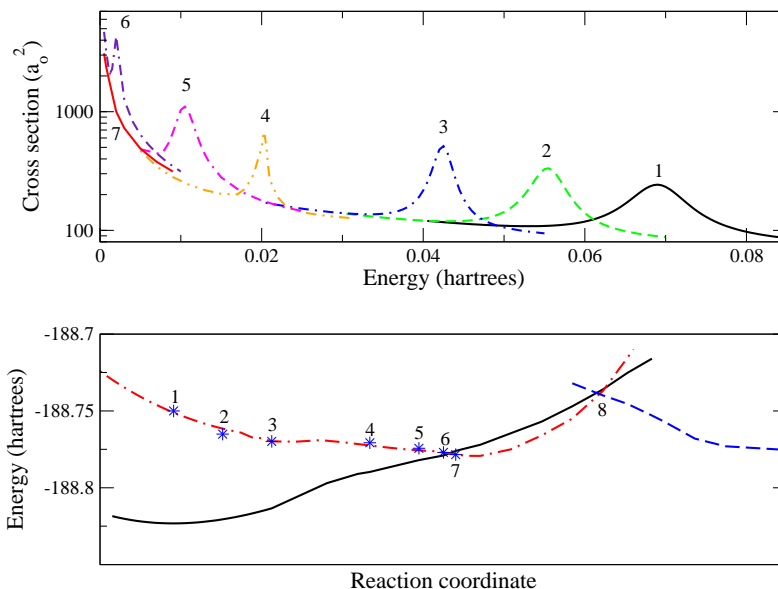


FIG. 4: (Color online) Fixed-nuclei cross sections and potential energy curves along a reaction path leading to $\text{HCOO}^- + \text{H}$. Upper panel: Fixed nuclei cross sections at seven different geometries. Lower panel: potential curves for neutral target (solid curve), π^* anion (dash-dot curve) and $2A'$ anion (dashed curve) along the reaction path. See text for detailed description of the geometry changes along the reaction path.

in the Kohn trial function $(N+1)$ -electron terms generated by singly exciting the occupied target orbitals into all unoccupied orbitals whose orbital energies were less than two hartrees, subject to the restriction that the three core orbitals (carbon and oxygen 1s) remain doubly occupied. In the results we report here, we used the triple-zeta contraction of the [9s,5p,1d] oxygen and carbon and [4s,1p] hydrogen gaussian basis sets given by Dunning [13], augmented with an additional diffuse p-function ($\alpha = .059$) on the oxygens. We also carried out calculations using smaller basis sets and found only small differences which in no way change our conclusions.

The equilibrium nuclear positions for the target in *trans* geometry [14] were optimized at the SCF level (see Fig. 1). Fixed-nuclei calculations at this geometry reveal an A'' resonance in the elastic cross section at ~ 1.9 eV with a width of ~ 0.2 eV. Fig. 2 shows the results of a series of calculations in which the C=O (carbonyl) bond distance is allowed to vary about its equilibrium value, while all other nuclear parameters are held fixed. The behavior is typical of what is seen with targets such as N_2 [15] or C_2H_4 [16]: a prominent resonance peak that decreases in energy and becomes narrower as the bond length increases. The anion curve, which is obtained by adding the resonance energy to that of the neutral target, forms a potential well that lies above that of the neutral and has its minimum displaced to a larger CO internuclear distance. The anion well can evidently support a number of quasi-bound vibrational levels.

Fig. 3 shows the behavior of the cross section in pla-

nar geometry as the OH bond is stretched, with the other nuclei again fixed at their equilibrium positions. In this case, there is relatively little change in the resonance energy as the OH distance is increased from its equilibrium value and the anion curve simply tracks that of the neutral target. As we stated earlier, dissociation cannot proceed along this path.

The key sequence of calculations that elucidate the dissociation mechanism are depicted in Fig.4. Seven sets of fixed-nuclei cross sections are shown. In the first four sets, with the molecule in planar geometry, we start at the equilibrium geometry (point 1 in Fig. 4) and then increase the C=O and C-O bond distances from their equilibrium values by 0.02, 0.04, 0.08 Å and 0.04, 0.08, 0.16 Å, respectively. In the last three sets (points 5, 6 and 7 in Fig. 4), the planar geometry is then broken by holding all the bond distances fixed while moving the hydrogen which is bonded to carbon out of the plane of the other nuclei by rotations about the C=O bond of 20° , 30° and 40° . In contrast to the previous two sequences shown, the anion energy decreases along this path as the resonance energy moves lower as well. The anion curve crosses the neutral curve, i.e. becomes electronically bound, when the hydrogen has been rotated out of plane by $\sim 35^\circ$, at which point the resonance feature is no longer visible in the fixed-nuclei cross section. Electronic structure calculations were then performed to track the anion energy at geometries where it is electronically bound. To maintain consistency with our scattering calculations, the structure calculations were performed using the same basis

sets and configurations as described above. If we start at the geometry where the anion curve crosses the neutral curve (point number 7 in Fig. 4) and increase the OH distance, the anion energy is found to increase monotonically and recrosses the neutral surface when the OH bond distance reaches ~ 1.3 Å (point 8 in Fig. 4). However, our calculations show that in this crossing region there are actually two *electronically bound* anion states (the dashed and dash-dot curves in Fig. 4). Electronic structure calculations produce adiabatic curves that do not cross, but for clarity, we have plotted the diabatic curves. We have verified that the lower state (dashed curve in Fig. 4), which we will refer to as $2A'$, correlates with $\text{HCOO}^- + \text{H}$ with increasing OH distance. Thus, DEA to the experimentally observed fragments appears to follow an adiabatic path on which the π^* state changes character and becomes the $2A'$ anion state. This occurs at the non-planar geometries where the two states are close in energy. We have not attempted to locate the precise geometry of the seam of intersection (or conical intersection) between the two anion surfaces, but we have shown that the energy in the crossing region is close to the anion energy at the equilibrium geometry of formic acid, i.e. the energies at points 1 and 8 in Fig. 4 are close.

The $2A'$ anion state has considerable s-wave character and, unlike the π^* state, produces no resonance features in the fixed-nuclei cross sections, even at geometries where its energy lies above that of neutral formic acid. We believe that at geometries where it is slightly unbound it has the character of a virtual state [17], which partially explains the large rise in the fixed-nuclei cross section at low energies [18]. The situation is complicated by the fact that formic acid is a polar molecule and the long-range electron-dipole interaction also leads to large cross sections at low energies. However, if the dipole interaction alone were responsible for this behavior, then the cross section at low energies would scale with the square of the target dipole moment [19]. By examining how the low-energy cross sections change with target geometry, we have verified that this is not the case.

A complete description of DEA for this molecule would require nuclear dynamics calculations involving accurate, complex-valued, multi-dimensional surfaces for both anion states, as well as non-adiabatic coupling elements, which is beyond the scope of this initial study. Nevertheless, our calculations give considerable insight into the observed nuclear dynamics for this system, which may have important implications for DEA in other biomolecules. Indeed, Allan has proposed a similar mechanism to explain his experimental study of electron interactions with chlorobenzene [20]. The path to stable formate ion fragments requires a symmetry-breaking, non-planar deformation of the negative ion state initially created by capture of a low energy electron at the equilibrium geometry of the target. We have identified a route to this region that is energetically downhill. But there is

an outer energy barrier on the path to dissociation that brings the anion energy close to its initial value. In this region, the electronic character of the anion changes, providing a direct path to the observed products. Since the DEA mechanism involves a barrier, it is likely that there would be considerable reflection of a wavepacket initially created on the π^* surface that would tend to keep part of it localized over the inner well. If a portion of the wavepacket persists for a time that is comparable to one or two vibrational periods before decay to autodetachment of the electron over the inner well, then this would explain why there is fine structure in the DEA cross section, since the time scales for complete dissociation and resonant vibrational excitation would be comparable.

The authors have benefitted from helpful discussions with Michael Allan. This work was performed under the auspices of the US Department of Energy by the University of California Lawrence Berkeley Laboratory under contract DE-AC02-05CH11231. The work was supported by the US DOE Office of Basic Energy Science, Division of Chemical Sciences. A.E.O. also acknowledges support from the National Science Foundation (Grant No. PHY-02-44911).

-
- [1] B. Boudaiffa, P. Cloutier, D. Hunting, M. A. Huels, and L. Sanche, *Science* **287**, 1658 (2000).
 - [2] J. Ellder *et al.* *Astrophys. J.* **242**, L93 (1980).
 - [3] W. M. Irvine *et al.* *Astrophys. J.* **342**, 871 (1989).
 - [4] A. Pelc, W. Sailer, P. Scheier, N. J. Mason, and T. D. Märk, *Eur. Phys. J. D* **20**, 441 (2002).
 - [5] A. Pelc *et al.*, *Chem. Phys. Lett.* **361**, 277 (2002).
 - [6] M. Tronc, M. Allan, and F. Edard, in *Abstracts of Contributed Papers, XV ICPEAC, Brighton* (1987).
 - [7] K. Aflatooni, B. Hitt, G. A. Gallup, and P. D. Burrow, *J. Chem. Phys.* **115**, 6489 (2001).
 - [8] V. Vizcaino, M. Jelisavcic, J. Sullivan, and S. J. Buckman, *Bull. Am Phys. Soc* **50**, 37 (2005).
 - [9] S. J. Buckman, private communication.
 - [10] M. Allan, private communication.
 - [11] F. A. Gianturco and R. R. Lucchese, *New J. Phys.* **6**, 66 (2004).
 - [12] T. N. Rescigno, B. H. Lengsfeld, and C. W. McCurdy, in *Modern Electronic Structure Theory*, edited by D. R. Yarkony (World Scientific, Singapore, 1995), vol. 1.
 - [13] T. H. Dunning, *J. Chem. Phys.* **53**, 2823 (1970).
 - [14] S. Leach *et al.*, *Chem. Phys.* **286**, 15 (2003).
 - [15] A. U. Hazi, T. N. Rescigno, and M. Kurilla, *Phys. Rev. A* **23**, 1089 (1981).
 - [16] C. S. Trevisan, A. E. Orel, and T. N. Rescigno, *Phys. Rev. A* **68**, 062707 (2003).
 - [17] J. R. Taylor, *Scattering Theory: The Quantum Theory of Nonrelativistic Collisions* (John Wiley & Sons, Inc., 1972), p. 246.
 - [18] D. Field, N. C. Jones, S. L. Lunt, and J.-P. Ziesel, *Phys. Rev. A* **64**, 022708 (2001).
 - [19] W. R. Garrett, *Mol. Phys.* **24**, 465 (1972).
 - [20] T. Skalicky, C. Chollet, N. Pasquier, and M. Allan, *Phys.*

Chem. Chem. Phys. 4, 3583 (2002).